Carbohydrate Polymers 120 (2015) 69–73

Contents lists available at ScienceDirect

Carbohydrate Polymers

journal homepage: www.elsevier.com/locate/carbpol

Structure–property relationships in *Sterculia urens*/polyvinyl alcohol electrospun composite nanofibres

Niranjan Patra*, Lenka Martinová, Martin Stuchlik, Miroslav Černík

Centre for Nanomaterials, Advanced Technologies and Innovation, Technical University of Liberec, Studentská 1402/2, Liberec 461 17, Czech Republic

ARTICLE INFO

Article history:
Received 1 August 2014
Received in revised form 2 December 2014
Accepted 5 December 2014
Available online 12 December 2014

Keywords:
PVA
Sterculia urens
Nanofibres
Deacetylation
Thermal properties
Crystallinity

ABSTRACT

Sterculia urens (Gum Karaya) based polyvinyl alcohol (PVA) composite nanofibres have been successfully electrospun after chemical modification of *S. urens* to increase its solubility. The effect of deacetylated *S. urens* (DGK) on the morphology, structure, crystallization behaviour and thermal stability was studied for spuned fibres before and after spinning post treatment. An apparent increase in the PVA crystallinity were observed in the PVA–DGK composite nanofibres indicating *S. urens* induced crystallization of PVA. The pure PVA nanofibre and the nanofibres of PVA–DGK composites were introduced to post electrospinning heat treatment at 150 °C for 15 min. The presence of sterculia gum reduced the fibre diameter and distribution of the nanofibres due to the increased stretching of the fibres during spinning. Switching of the thermal behaviour occurs due to post spinning heat treatments.

1. Introduction

In the scientific community there are several different methods used to produce nanostructures in which the electrospinning technique is one of the most popular, easy and economical to produce nanofibres of different properties and applications (Reneker & Chun, 1996; Li & Xia, 2004; Teo & Ramakrishna, 2006). In this technique the polymer is dissolved in a suitable solvent and the polymer solution is spun to a nanometre scale under the influence of a strong electrical field. The fibre spinning process takes a fraction of a millisecond to stretch and deposit on the substrate with a very high aspect ratio. These types of nanofibres have many applications in different fields (Ramakrishna, Mayer, Wintermantel, & Leong, 2001; Agarwal, Wendorff, & Greiner, 2008; Barakat et al., 2010; Inagaki, Yang, & Kang, 2012).

Tree gum exudates of the natural acid polysaccharide have attracted significant attention among researchers because of their immense potential application in the food industry, biomedicine and material science (de Paula & Rodrigues, 1995; de Paula, Santana, & Rodrigues, 2001; Ibrahim, Abo-Shosha, Allam, & El-Zairy, 2010; Kumar & Ahuja, 2012; Le Cerf, Irinei, & Muller, 1990; Patra et al, 2014; Singh & Sharma, 2009; Verbeken, Dierckx, & Dewettinck, 2003). Natural acid polysaccharides are inexpensive, easily available, non-toxic, biodegradable materials which exhibit peculiar physicochemical properties and applications (Verbeken et al., 2003; Vinod, Sashidhar, Sarma, & Vijaya Saradhi, 2008; Vinod & Sashidhar, 2010). Among the different tree gum polysaccharides, Gum Karaya (GK) is an important partially acetylated natural polysaccharide having a branched structure with a high molecular mass of 16×10^6 Da and is grouped under the substituted rhamnogalacturonoglycan (pectic) type of tree gum. GK is mainly composed of acidic and neutral sugars like galactose (13–26%) and rhamnose (15–30%), which is different compared to other gum tree exudates. However, the protein content of GK is less than other gum exudates. GK is commonly used for food and non-food applications due to its acid stability, high viscosity and good suspension properties (Verbeken et al., 2003).

Of the many different thermoplastic semi-crystalline polymers, PVA is one of the most used hydrophilic polymers for electrospinning due to the presence of a hydroxyl group in its ever-repeating unit which makes it cross-linkable. The composites of PVA and GK have received attention because of their excellent viscosity and gelling properties (Singh & Pal, 2008). However, work focused on the preparation of nanofibres and the subsequent characterization of their biomedical applications (Li & Xia, 2004; Ramakrishna et al., 2001; Reneker

* Corresponding author. Tel.: +420 48 5353835.
E-mail addresses: patraji@gmail.com, patrasaheb@gmail.com (N. Patra).

http://dx.doi.org/10.1016/j.carbpol.2014.12.002
0144-8617/

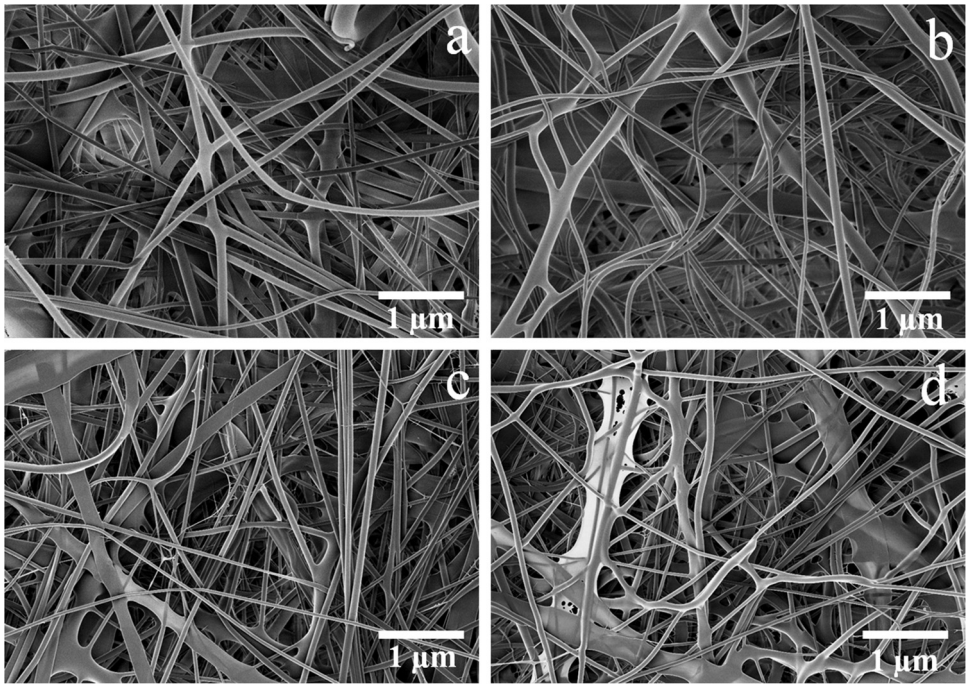

Fig. 1. SEM images of the PVA and PVA–DGK composites nanofibres (a) PVA NX (b) PVA X (c) PVA–DGK 2 NX (d) PVA–DGK 2 X.

& Chun, 1996; Teo & Ramakrishna, 2006), the fundamental understanding of the structural property relation within composite nanofibres and their effect on the fibre properties is still lacking.

In this study, deacetylated Gum Karaya (DGK) was used to prepare biodegradable and biocompatible composite nanofibres with PVA. In order to see the effects of DGK on the structure, morphology, crystallinity, and thermal stability of the composite fibres,

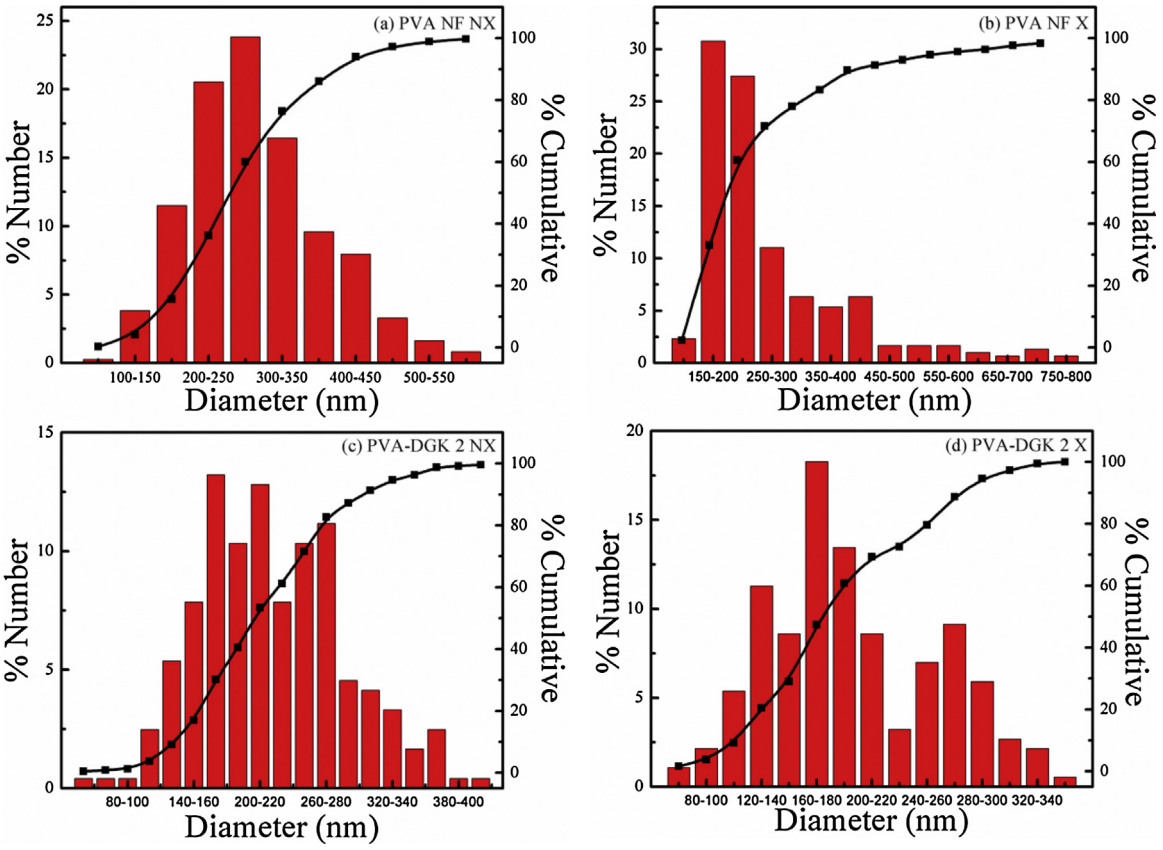

Fig. 2. The fibres diameter distribution histogram of (a) PVA NX (b) PVA X (c) PVA–DGK 2 NX (d) PVA–DGK 2 X.

the fibres were studied and compared with the pure PVA fibres. Post electrospinning treatment by heat is also discussed. This study will contribute to an understanding of the action of polymer matrix and filler–matrix interactions in PVA–DGK composite fibres which may find may find excellent applications in biomedical science.

2. Experimental details

2.1. Materials and methods

PVA of an average molecular weight of ~125,000 g mol^{-1} (98% hydrolyzed), *Sterculia urens* (Gum Karaya), hydrochloric acid (HCl) 35%, and sodium hydroxide (NaOH) were obtained from Sigma-Aldrich. Distilled water (MERK Milli-Q Advantage A10) was used for dissolving the GK.

2.2. Deacetylation reaction

For the deacetylation reaction, GK of 1 wt% was taken in a glass beaker with 100 mL of water. The gum solution was stirred with the help of a magnetic stirrer at 40 °C. Deacetylation was carried out at a pH of 10 by adding appropriate amount of NaOH solution. The solution was filtered using a sintered filter (Sintered Glass Buchner Funnel) to remove any foreign particles and dirt. Then, the DGK solution was precipitated using ethanol, centrifuged and the precipitate was dried at a temperature of 40 °C for 24 h using an air dryer. The dried deacetylated GK was later crushed to powder in a ceramic mortar. This modified deacetylated GK was designated as the DGK sample.

2.3. Electrospinning of PVA and PVA–DGK composite nanofibres and heat treatment

Pristine PVA and PVA–DGK composite nanofibres were fabricated by a laboratory pilot plant spinner NANOSPIDER (ELMARCO, Czech Republic) using a continuous moving head in a wire with a static spunbond from a polypropylene fibre collector (thickness of the spunbond 0.125 ± 0.015 mm, surface mass 21.1 ± 3 g m^{-2}, applied electrical potential 60 kV). The distance between the spinning head of the wire and the collector was 15 cm. An aqueous solution of 11 wt% PVA containing 2 wt% GK (by PVA weight) was used for the electrospinning. The temperature and the relative humidity during the electrospinning were around 20 °C and 37%, respectively. Pristine PVA nanofibres were also electrospun from 11 wt% PVA solution under the same operating conditions. The produced nanofibres were exposed to heat treatment at 150 °C for 15 min. The samples were labelled PVA–DGK-number-X/NX, where the number is based on the wt% DGK used, X represent heat treatment and NX represent no treatment.

2.4. Characterization

The morphology of the electrospun nanofibres was observed under a scanning electron microscope (SEM) (Carl ZEISS Ultra/Plus, Germany). The fibre diameter were calculated by the image analysis software NES. DSC measurements were carried out on a calorimeter (Mettler Toledo) between 0 and 250 °C with a ramping rate of 10 °C min^{-1} operating in a nitrogen (N_2) atmosphere with a flow rate of 20 mL min^{-1}. Approximately 5 mg of sample crimped in an aluminium pan was used for the experiment. The DSC instrument was calibrated based on the melt onset and heat of fusion of indium at 156.6 °C, with a value of 28.4 J g^{-1} as the standard material. FT-IR spectra of pristine PVA powder, GK, DGK and composite nanofibres were acquired in the range of 680–4000 cm^{-1} using a NICOLET iS10 (Thermo scientific Co. USA) in total attenuated reflection mode. All the spectra were baseline corrected by the 2nd order polynomial and were normalized thereafter with the highest peak. Thermal stability of the material was determined using a TGA/SDTA851 (Mettler Toledo) thermogravimetre in an N_2 atmosphere at a flow rate of 60 mL min^{-1}. About 11 mg of sample was heated from 30 to 600 °C with the heating rate of 10 °C min^{-1}. X-ray diffraction (XRD) patterns were obtained using a computer controlled (PANalytical Xpert^3) X-ray diffractometer using Cu $K\alpha 1$ radiation (λ = 1.540598 Å). The X-ray tube was operated at 40 kV, 40 mA with step scanning technique at a step width of 0.030 (2θ).

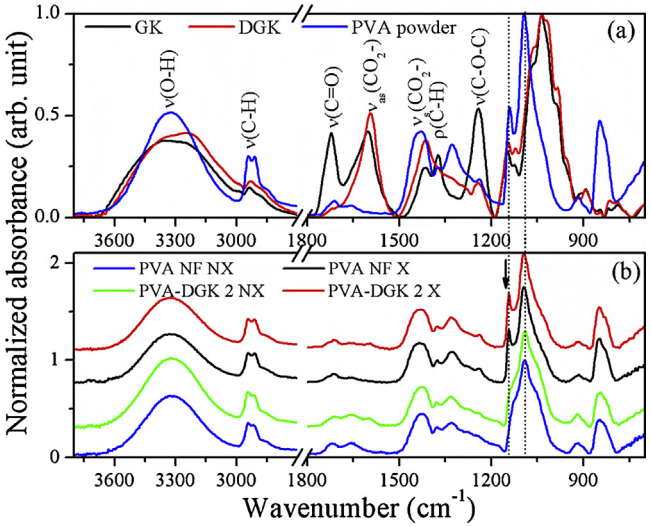

Fig. 3. Normalized ATR–FT-IR spectra of (a) pristine GK, DGK and PVA powder (b) PVA and PVA–DGK composites nanofibres before and after heat treatment.

3. Results and discussion

Fig. 1 shows SEM micrographs of pristine PVA and PVA–DGK composite nanofibres before and after heat treatment, respectively. The SEM micrographs are very uniform and free of microbeads (which are due to variation in relative humidity and process temperature) for all of the pristine and composite nanofibres. The PVA nanofibres have an average diameter of 290 nm whereas the diameter of the composite nanofibres reduces considerably (Fig. 2 and Table 1). The fibre diameter distribution is very narrow for the composites nanofibres (Fig. 2). The reduced nanofibres diameter for the composites fibres is due to the increase in crystallinity and the presence of DGK which increases the stretching due to higher charge density. After heat treatment of the nanofibres at 150 °C the average fibre diameter and uniformity of the nanofibres again decreases.

Fig. 3(a) shows the normalized FT-IR absorption spectral band of pristine GK, DGK and PVA powder. The major bands observed for GK correspond to the vibrations of the characteristic groups. The broad band at 3370 cm^{-1} corresponds to the O—H stretching band of the hydroxyl group of the galactopyranose and glucopyranose ring; 1725 cm^{-1} to the stretching vibration of C=O; 1595 cm^{-1} to the C=C band and/or CO_2^- asymmetric stretching vibration from carboxylic acid salts; 1417 and 1371 cm^{-1} represent the C—H deformation bands and also in this part of the spectrum the CO_2^- symmetric stretching vibration from carboxylic acid salts can be found. The band at 1244 cm^{-1} is due to the ester C—O—C stretching vibration and intensity of the band decreased after deacetylation. In the case of the deacetylation reaction, we found that the major O—H stretching band shifted to lower frequencies than the pristine GK. The deacetylation procedure also eliminated the CO—C ester bond, the carbonyl group from the ester and made changes in the deformation and skeletal vibrations e.g. C—H deformation bands. The degree of deacetylation calculated for the DGK is ~98%.

Table 1
DSC results i.e. melting point, enthalpy, and crystallinity.

Sample	Fibre diameter (nm)	T_{onset} (°C)	T_m (°C)	$Area_{mp}$ (mJ)	ΔH (J g^{-1})	Crystallinity (%)
PVA powder	–	204	220	396	75	48.3
PVA NF NX	290	211	221	278	54	34.8
PVA NF X	270	211	218	264	50	32.2
PVA–DGK 2 NX	220	214	224	381	73	47.0
PVA–DGK 2 X	190	214	223	402	78	50.3

Fig. 3(b) shows the normalized FT-IR absorption spectra of PVA and PVA–DGK composite nanofibres before and after heat treatment, respectively. The broad band at 3300 cm^{-1} corresponds to the O—H stretching band of the hydroxyl group; 2943 and 2906 cm^{-1} to the C—H stretching band; 1725 cm^{-1} to the C=O stretching vibration; 1608 cm^{-1} to the C=C band and/or CO_2^- stretching vibration from carboxylic acid salts for the DGK; 1421 and 1373 cm^{-1} represent the C—H deformation band, 1421 cm^{-1} is a hidden CO_2^- band and the band at 1244 cm^{-1} is due to C—O—C stretching.

By comparing the spectra, the intensity of the broad band at 3300 cm^{-1}, which is for the hydroxyl band, increases and broadens for the PVA–DGK nanofibres. These increases in intensity of PVA–DGK suggest that the hydrogen bonding becomes stronger. The important band at 1142 cm^{-1} of the PVA structure suggests a semi-crystalline synthetic polymer able to form certain domains depending on the process parameters and the blended materials. The band at 1142 cm^{-1} in pristine PVA becomes broader in the PVA–DGK complex, which can be attributed to the alcohol (C—O band) and the acetyl (C—O—C bands) formed by the reaction of PVA with DGK. Similarly, the peak intensity at 1651 cm^{-1} increase in case of the PVA–DGK, indicating a possible formation of acetyl bridges compared to the pristine PVA.

Fig. 4 shows the DSC heating curve of pristine PVA powder, PVA and PVA–DGK 2% composites nanofibres before and after heat treatment, respectively. In order to see the consistency and reproducibility, three measurements for each sample were performed and averaged. As we can see in the case of the PVA powder a broad peak appeared at around 144 °C, which is due to the adsorbed solvent or moisture release from the pristine PVA.

The onset of the melting peak of the PVA powder started at 204 °C as indicated in Table 1. In case of the PVA powder the height of the melting peak is lower. In case of nanofibres, the broad peak at 144 °C disappears due to crystallization, which occurs due to the presence of the DGK. In case of nanofibres the broad peak of water or entrapped solvent during the spinning appears at a lower temperature of around 60 to 76 °C. Interestingly, we found that the broad peak which appears for the PVA powder does not appear for the nanofibres at 144 °C, which again comes after the heat treatment of the samples, which we can see in Fig. 4. Even after the heat treatment of the nanofibres the broad peak at 47 °C is still there due to the water absorption capacity of the GK.

PVA is a semi crystalline polymer with an amorphous phase. The overall crystalline content depends on the molecular weight and the molecular weight distribution, degree of branching, and filler content. The PVA material property depends on the crystalline content. The crystallinity was determined from the ΔH values obtained from the area under the melting peak with a theoretical value for 100% crystalline PVA which is 155 J g^{-1} (Probst, Moore, Resasco, & Grady, 2004). The pristine PVA nanofibres have a crystallinity of 32–35%, whereas for the PVA–DGK 2% composites nanofibres it increases to 47% and then to 50–51% after the heat treatment of the composite nanofibres. The pure PVA nanofibres exhibited lower crystallinity compared to the composite nanofibres as calculated from the numerical integration of the area under the melting peak, taking into account 155 J g^{-1} as the standard value for a 100% crystalline PVA. The observed increase in crystallinity is due to the DGK.

Wide angle X-ray diffraction was used to study the PVA crystallization in both PVA and PVA–DGK composite nanofibres. As seen in Fig. 5, the diffraction peaks for the PVA nanofibres without heat treatment appeared at $2\theta = 19.5°$ (1 0 1) planes of semi crystalline PVA (Assendert & Windle, 1998). The (1 0 1) plane was the main crystalline phase due to the high integrated area.

For the PVA–DGK composite nanofibres change in the (1 0 1) diffraction intensity and emergence of the (0 0 1) and (2 0 0) planes occurs. Upon comparison of PVA nanofibres with the PVA–DGK composite nanofibres led to stronger (1 0 1) and (2 0 0) reflection and the emergence of medium intensity (0 0 1) reflections planes at

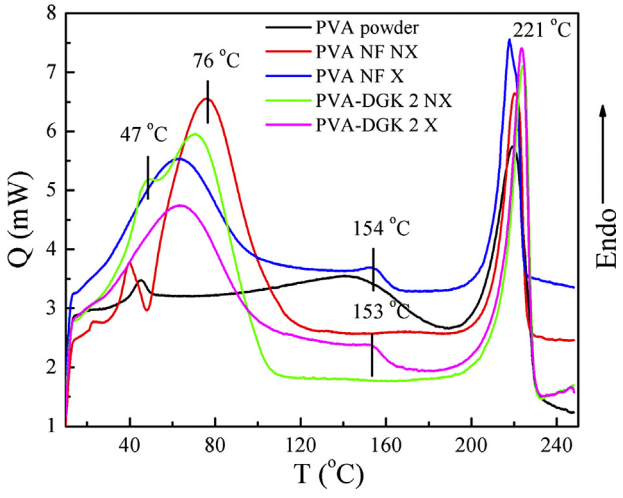

Fig. 4. DSC of PVA powder, PVA and PVA–DGK 2% nanofibres before and after heat treatment.

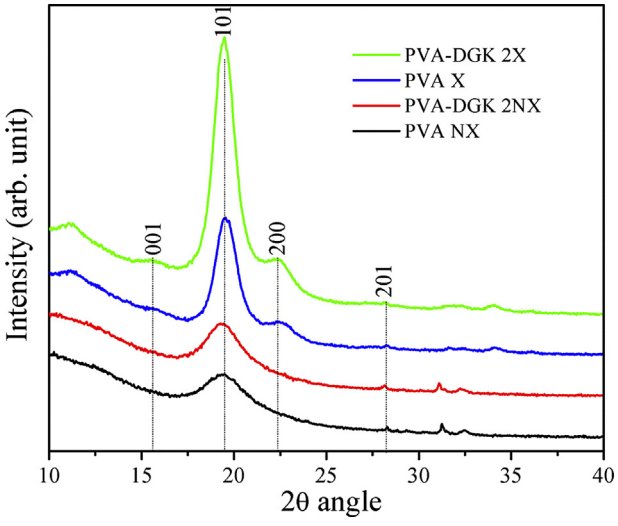

Fig. 5. XRD patterns of PVA and PVA–DGK 2% composite nanofibres before and after treatment.

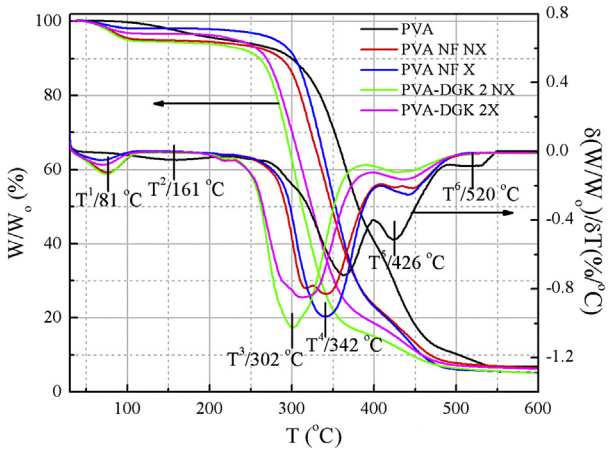

Fig. 6. TG–DTG plot of PVA powder, PVA nanofibres and PVA–DGK 2% composite nanofibres before and after heat treatment.

16.0°. However, when the nanofibres were heat treated, the (1 0 1) reflection intensity was increased.

The PVA–DGK composite nanofibres showed peak at $2\theta = 19.5°$ with high intensity indicating a DGK induced change in the main crystalline phase of PVA which is believed to be due to the confinement of DGK in PVA macromolecular chains within the nanofibres. The post electrospinning treatments influenced diffraction patterns for both the pure PVA and PVA–DGK composite nanofibres. For PVA nanofibres, after heat treatment emergence of (0 0 1) and (2 0 0) planes. For the PVA–DGK composite nanofibres, the post electrospinning heat treatments increased the intensity of the (0 0 1), (1 0 1) and (2 0 0) planes. This suggested that the presence of DGK plays an important role in PVA crystallinity.

Fig. 6 shows the thermogravimetric and differential thermogravimetry plot of pristine PVA powder, pristine PVA nanofibres, PVA–DGK 2% composites nanofibres before and after heat treatment which gives instant information about the thermal stability and water/solvent retention of the materials (Patra et al., 2012). From the TGA plot we can see that the pristine PVA powder decomposes in two major steps. The broad peak for the PVA powder at around 161 °C is due to the removal of the moisture and solvent in the original material which is higher than the spun nanofibres. The maximum weight of the solvent in the PVA powder is around 10%. In the case of all of the nanofibres, the weight loss is due to the retained water which is removed at around 81 °C i.e. at a lower temperature than the PVA powder. The major degradation peak occurs at around 302 °C which is for the PVA–DGK 2 NX. We determined that the area under the second degradation peak is less for all of the nanofibres than for the PVA powder. In case of PVA powder, pristine PVA nanofibres, PVA–DGK 2% composite nanofibres after the heat treatment the entrapped moisture and solvent reduced to 4% and the DTG peak T^1 appears at around 81 °C. There is little change in the peak position of the DTG compared to the untreated nanofibres. The T6 peak area decreases considerably.

4. Conclusions

A composite based on *S. urens* and PVA was successfully electrospun into nanofibres. We have demonstrated that DGK has a major role on the structure, crystallinity and morphology of the composites nanofibres even at a very small amount of 2%. The DGK caused an apparent increase in crystallinity. The cystallinity can be further improved by the heat treatments of the nanofibres for 15 min. The SEM confirmed the composite nanofibres are uniform and free of microbeads, and have a smaller diameter, which is probably due to the increase in crystallinity and the stretching due to higher charge density. These results suggest that the crystallinity of the PVA nanofibres can be tuned by adding a small amount of DGK. PVA that is able to form nucleation crystallization with DGK would serve to develop biodegradable, biocompatible low cost composites nanofibres for the application in biomedical or material science.

Acknowledgements

The results of this project LO1201 were obtained through the financial support of the Ministry of Education, Youth and Sports in the framework of the targeted support of the "National Programme for Sustainability I", the OPR&DI project Centre for Nanomaterials, Advanced Technologies and Innovation CZ.1.05/2.1.00/01.0005 and the Project "Development of Research Teams of R&D Projects at the Technical University of Liberec" No. CZ.1.07/2.3.00/30.0024.

References

Agarwal, S., Wendorff, J. H., & Greiner, A. (2008). Use of electrospinning technique for biomedical applications. *Polymer*, *49*(26), 5603–5621.

Assendert, H. E., & Windle, A. H. (1998). Crystallinity in poly(vinyl alcohol). 1. An X-ray diffraction study of atactic. *PVOH*, *39*(18), 4295–4302.

Barakat, N. A. M., Abadir, M. F., Sheikh, F. A., Kanjwal, M. A., Park, S. J., & Kim, H. Y. (2010). Polymeric nanofibres containing solid nanoparticles prepared by electrospinning and their applications. *Chemical Engineering Journal*, *156*(2), 487–495.

de Paula, R. C. M., & Rodrigues, J. F. (1995). Composition and rheological properties of cashew tree gum, the exudate polysaccharide from *Anacardium occidentale* L. *Carbohydrate Polymers*, *26*(3), 177–181.

de Paula, R. C. M., Santana, S. A., & Rodrigues, J. F. (2001). Composition and rheological properties of *Albizia lebbeck* gum exudate. *Carbohydrate Polymers*, *44*(2), 133–139.

Ibrahim, N. A., Abo-Shosha, M. H., Allam, E. A., & El-Zairy, E. M. (2010). New thickening agents based on tamarind seed gum and karaya gum polysaccharides. *Carbohydrate Polymers*, *81*(2), 402–408.

Inagaki, M., Yang, Y., & Kang, F. (2012). Carbon nanofibres prepared via electrospinning. *Advanced Materials (Deerfield Beach, Fla.)*, *24*(19), 2547–2566.

Kumar, A., & Ahuja, M. (2012). Carboxymethyl gum kondagogu: Synthesis, characterization and evaluation as mucoadhesive polymer. *Carbohydrate Polymers*, *90*(1), 637–643.

Le Cerf, D., Irinei, F., & Muller, G. (1990). Solution properties of gum exudates from *Sterculia urens* (Karaya gum). *Carbohydrate Polymers*, *13*(4), 375–386.

Li, D., & Xia, Y. (2004). Electrospinning of nanofibres: Reinventing the wheel? *Advanced Materials*, *16*(14), 1151–1170.

Patra, N., Jayaseelan, D. D., & Lee, W. E. (2014). Synthesis of biopolymer-derived zirconium carbide powder by facile one-pot reaction. *Journal of the American Ceramic Society*, http://dx.doi.org/10.1111/jace.13321

Patra, N., Salerno, M., Cozzoli, P. D., Barone, A. C., Ceseracciu, L., Pignatelli, F., Carzino, R., Marini, L., & Athanassiou, A. (2012). Thermal and mechanical characterization of poly(methyl methacrylate) nanocomposites filled with TiO_2 nanorods. *Composites Part B: Engineering*, *43*(8), 3114–3119.

Probst, O., Moore, E. M., Resasco, D. E., & Grady, B. P. (2004). Nucleation of polyvinyl alcohol crystallization by single-walled carbon nanotubes. *Polymer*, *45*(13), 4437–4443.

Ramakrishna, S., Mayer, J., Wintermantel, E., & Leong, K. W. (2001). Biomedical applications of polymer-composite materials: A review. *Composites Science and Technology*, *61*(9), 1189–1224.

Reneker, D. H., & Chun, I. (1996). Nanometre diameter fibres of polymer, produced by electrospinning. *Nanotechnology*, *7*(3), 216–223.

Singh, B., & Pal, L. (2008). Development of sterculia gum based wound dressings for use in drug delivery. *European Polymer Journal*, *44*(10), 3222–3230.

Singh, B., & Sharma, N. (2009). Mechanistic implication for cross-linking in sterculia-based hydrogels and their use in GIT drug delivery. *Biomacromolecules*, *10*(9), 2515–2532.

Teo, W. E., & Ramakrishna, S. (2006). A review on electrospinning design and nanofibre assemblies. *Nanotechnology*, *17*(14), R89–R106.

Verbeken, D., Dierckx, S., & Dewettinck, K. (2003). Exudate gums: Occurrence, production, and applications. *Applied Microbiology and Biotechnology*, *63*(1), 10–21.

Vinod, V. T. P., & Sashidhar, R. B. (2010). Surface morphology, chemical and structural assignment of gum Kondagogu (*Cochlospermum gossypium* DC.): An exudate tree gum of India. *Indian Journal of Natural Products and Resources*, *1*(2), 181–192.

Vinod, V. T. P., Sashidhar, R. B., Sarma, V. U. M., & Vijaya Saradhi, U. V. R. (2008). Compositional analysis and rheological properties of gum kondagogu (*Cochlospermum gossypium*): A tree gum from India. *Journal of Agricultural and Food Chemistry*, *56*(6), 2199–2207.